5-1-2020

Differential Gene Expression of Human Renal Proximal Tubule Cells Exposed to Biologically Relevant Fluid Shear Stress

Hanna Yvonne Sothers

Differential Gene Expression of Human Renal Proximal Tubule Cells Exposed to Biologically Relevant Fluid Shear Stress

by

Hanna Yvonne Sothers

An Honors Capstone
submitted in partial fulfillment of the requirements
for the Honors Diploma
to
The Honors College
of
The University of Alabama in Huntsville

02/03/19

Honors Capstone Director: Dr. Luis Cruz-Vera First Last

Associate Professor of Biology Department

Student **Date**

05/01/2020

Director **Date**

05/02/2020

Department Chair **Date**

Honors College Dean **Date**

HONORS COLLEGE
THE UNIVERSITY OF ALABAMA IN HUNTSVILLE

Honors College
Frank Franz Hall
+1 (256) 824-6450 (voice)
+1 (256) 824-7339 (fax)

honors@uah.edu

Honors Thesis Copyright Permission

This form must be signed by the student and submitted as a bound part of the thesis.

In presenting this thesis in partial fulfillment of the requirements for Honors Diploma or Certificate from The University of Alabama in Huntsville, I agree that the Library of this University shall make it freely available for inspection. I further agree that permission for extensive copying for scholarly purposes may be granted by my advisor or, in his/her absence, by the Chair of the Department, Director of the Program, or the Dean of the Honors College. It is also understood that due recognition shall be given to me and to The University of Alabama in Huntsville in any scholarly use which may be made of any material in this thesis.

Hanna Sothers
Student Name (printed)

Student Signature

5/1/2020
Date

Table of Contents

Abstract

Fluid shear stress (FSS) is a vital characteristic needed in order to recapitulate the microenvironment that proximal tubule cells (PTC) experience *in vivo*. Microfluidic devices are a promising model for this as they allow the PTCs to form a lumen through which a filtrate can pass. To show the importance of FSS, differential gene expression was measured between human renal proximal tubule cells (RPTEC/TERT-1) exposed FSS and those not.

The analysis found that over 10,000 genes had a significant change in expression when exposed to FSS, both upregulation and downregulation. About 330 of these genes had a highly significant change in expression and of those 69 have been previously implicated in the literature as being important to proximal tubule function. To further establish this, the gene expression of the transport proteins MRP2, MRP4, and BCRP were analyzed using PCR.

The "organ-on-a-chip" model is promising for future renal research. This model better mimics the environment that PTCs are found *in vivo*, especially in regards to lumen formation and the ability to replicate biologically relevant FSS. The device itself is also cost-effective and efficient, making it easier to standardized data between different studies.

Introduction

In 2017, kidney disease was the ninth leading cause of death in the United States (Heron, 2019). This is further characterized as nephritis (inflammation of the nephrons) or nephrosis/nephrotic syndrome (increased protein in the urine). These cause a loss of function of the kidneys, which are responsible for filtering waste from the body. Kidney disease can also be defined by how rapidly symptoms appear. Acute kidney injury (AKI) is the sudden loss of function due to drugs, injury, or etc and is reversible. Chronic kidney disease (CKD) is when the symptoms develop over a period of months or years and is not reversible. In either case, it can progress to renal failure and eventually death. Both AKI and CKD work to compound the effects of each other with CKD putting patients at an increased risk for AKI and with research showing AKI is an accelerator for CKD (Hsu & Hsu, 2016). In addition to this, certain drugs and therapies have also been shown to cause AKI (Shahrbaf & Assadi, 2015).

The kidneys are composed of a complex network of blood vessels and nephrons. Nephrons are the functional units of the kidney. They consist of a glomerulus and multiple sections of tubules. These sections are the proximal tubule (PT), the loop of Henle, and the distal tubule. The PT is the first section after the glomerulus and is a highly active site for reabsorption and secretion that plays a key part in kidney-drug interaction (Nakamura et al., 2014). This is because renal drug transporters are primarily localized to the proximal tubule cells (PTCs)(Yin & Wang, 2016). These cells are the first to come into contact with glomerular filtrate, making them more likely to come into contact with potentially nephrotoxic compounds. In addition to this, these cells have high quantities of mitochondria, low capacity for anaerobic ATP production, and very few antioxidant defenses which make PTCs susceptible to injury (Chevalier, 2016). Due to these factors, the PT is a prime area to conduct in vivo drug and therapy studies.

Previous research on the proximal tubule has been based on a two-dimensional (2D) model that does not recapitulate the *in vivo* microenvironment. However, since the late 90's the use of three dimensional (3D) models has risen (Velve-Casquillas et al., 2010). In the nephron,

PTCs form a lumen through which a filtrate passes through, generating fluid shear stress (FSS) or flow. Microfluidic devices are a promising 3D model for PTs since the cells are exposed to a microenvironment that better mimics that found *in vivo*. Particularly, the ability to recreate FSS. In other 3D models, PTCs have been demonstrated to recapitulate *in vivo* morphology and function better than under static, non-flow conditions (King et al., 2017). More research is needed to confirm the efficacy of this model, including the effects FSS may have on the gene and protein expression of human transporters. This would provide a crucial step in the development of a biologically relevant method for research on PTs.

We are interested in the effects FSS has on the overall gene expression of PTCs. To explore this, RPTEC-TERT1 cells were seeded into a microfluidic device and exposed to FSS for a period of 24 hours. RNA-sequencing (RNAseq) was used to observe the changes between cells exposed to flow (treatment) versus cells that were not (non-treatment). In addition to this, the expression levels for the genes ABCG2 (BCRP), ABCC2 (MRP2), and ABCC4 (MRP4) were further examined in RPTEC-TERT1 and HEK-293T cells. These genes code for ATP binding cassette (ABC) transport proteins that are known to be expressed on the apical side of the cells (Aschauer et al., 2015). This is an essential aspect in establishing the efficacy of microfluidic devices as a model for the human PT, which will be used in pharmaceutical and physiological assays.

Genomic

Introduction

To observe global transcriptome changes between static and flow environments, we used RNAseq. This is a type of whole-genome shotgun sequencing that allows for the mapping and quantifying of the transcriptome (Wang et al., 2009). In general, the process takes cDNA fragments or "reads" and aligns them to a reference genome. These reads are known as the library. The number of reads that align to a specific section of the genome allow us to make observations about which genes are more highly transcribed than others.

The first step in RNAseq is to create the cDNA library. To start this process, the RNA must first be collected from cells. After the total RNA is collected, mRNA is extracted from it. The mRNA is then fragmented and converted into cDNA. The last two steps can be swapped, converting to cDNA first then fragmenting (Hrdlickova et al., 2017). This, however, is not as straightforward and requires more precision so it is less common. Next, adapter sequences are added to each end of the fragments. These sequences will vary between platforms and may contain elements that help identify the ends of the cDNA. It is then amplified using PCR to ensure there are enough reads to get adequate data. At this point, the library is ready to be sequenced.

After the library has been sequenced, it is ready for analysis. First, the reads need to be processed. They have to be identified, the adapter sequences removed, and filtered by quality. Once that has been done, the reads must be normalized. This removes any outliers that would otherwise skew the data. The reads are aligned to a reference genome and matched to known gene loci. Then the aligned reads are then counted and normalized. One way of doing this is to use the quantiles associated with the raw reads as a scaling factor, as is the case with DESeq (Anders & Huber, 2010). After this, the data can be used in further statistical analysis relevant to the person doing the research.

For the purpose of this project, we were interested in any changes in the transcriptome of PTCs exposed to FSS versus those exposed to static conditions. Fluid Shear Stress has been previously implicated in the upregulation of vital PT transporters in animal models (Snouber et al., 2012). It is important in proving the efficacy of the microfluidic model of the human PT to show that gene expression changes when the cells are exposed to biologically relevant conditions.

To test this, we seeded RPTEC-TERT1 cells into linear microfluidic channels and exposed them to static conditions or one of three different FSS rates(0.5 dynes/cm^2 , 0.25 dynes/cm^2, or 0.1 dynes/cm^2). The first is considered to be the "normal" rate passing through a healthy nephron and the other two are considered to be "disease" states as they reflect a lower glomerular filtration rate which is associated with many forms of kidney disease (Ferrell, Cheng, Miao, Roy, & Fissell, 2018). These cells were then harvested and their total RNA sent to the HudsonAlpha Genomic Service Lab (https://gsl.hudsonalpha.org/information/rna), who made the libraries. Sequencing was performed on an Illumina HiSeq 2500 using paired-end reads of 50 bases (Illumina, San Diego, CA, USA). The sequenced library was then sent through aRNApipe, which is a pipeline for processing RNAseq output (Alonso et al., 2017). Genes that fell within the range $\log_2$ Fold Change ($\log_2$FC) > ± 0.4 and adjusted p-value (p-adjust) < 0.05 were considered to be significantly changed. If the p-adjust < 1x10^{-30} then the gene was considered to be highly differentially expressed, these were the genes that we focused on for the literature review.

Methods

Treatment

RPTEC-TERT1 cells were seeded into linear channels onto microfluidic devices, such as this one, that were coated in a collagen-1

Figure 1: *SynVivo* linear channel microfluidic device

matrix. The cells were then exposed to a flow rate of static(control) , 0.1 dynes/cm^2, 0.25 dynes/cm^2, or 0.5 dynes/cm^2 for a 24 hour period. Each device had at least one control channel and the other two being exposed to flow, which was randomly determined. After 24 hours, the cells were harvested and their genomic material was extracted. The total RNA was isolated using the ReliaPrep™ RNA Miniprep Systems (Z6011, Promega) per the manufacturer's instructions. The quality of the RNA was determined before sending it to the HudsonAlpha Genomic Service Lab for library preparation and sequencing. Concentration was measured by Qubit and integrity was measured using a 2100 Bioanalzyer. Samples that did not have an RNA integrity between 8.8 and 9.8 were excluded.

Computer Work

We compared the FSS conditions from each chip to the control (static) channels on the same device. There were 12 FSS samples and 10 static samples. The output from RNAseq as sent through aRNApipe (v1.1). The reads were trimmed with TrimGalore (http://www.bioinformatics.babraham.ac.uk/projects/trim_galore/) then aligned with STAR (v2.5.2b) (DOBIN) using the hg37 reference genome. Picard (https://broadinstitute.github.io/picard/) was used to assess the quality control metrics during the alignment process. Data analysis was performed in RStudio (v1.1.453) using R version 3.3.1. Gene expression changes were examined using the DESeq2 package (v1.12.4) (Love) with the default settings in likelihood ratio test mode (Marioni, Mason, Mane, Stephens, & Gilad, 2008) to calculate the differential expression. The R packages biomaRt (v.2.28.0)(Durinck et al., 2009) and biomartr (v.0.7.0) were used to convert the gene IDs to their ENSEMBL IDs. To create the volcano plot, the R packages ggplot2 (v. 3.0.1), edgeR (v.3.14.0),ggfortify (v.0.4.4) were used.

We generated a volcano plot that compared the negative $\log_{10}$ values from the differential expression analysis with the $\log_2$FC for each gene. Each point represents a discrete gene, those highlighted in red were identified in the literature.

Genes that fell within the range $\log_2 FC > \pm 0.4$ and p-adjust < 0.05 were considered to be significantly changed. Genes with a p-adjust $< 1x10^{-30}$ were considered to be highly significantly changed and were included in the literature search.

Literature Search

Only genes that fell within the cutoff range of $\log_2FC > \pm 0.4$ and p-adjust $< 1x10^{-30}$ were included in the literature search. This search limited results to papers from Pubmed that showed a gene's function in the PT or the kidney as a whole. Papers were limited to those that are available on Pubmed for quality control purposes.

Results

This project consisted of a literature review of the genes with significant changes in expression between treatment and non-treatment. The normalized expression as determined by DEseq2 showed that 10442 genes fell within the significantly changed range ($\log_2FC > \pm 0.8$ and p-adjust < 0.05). Of those, 337 fell within the highly significant range ($\log_2FC > \pm 0.8$ and p-adjust $< 1x10^{-30}$). The literature review identified 69 genes as being related to PTCs and their structure or function.

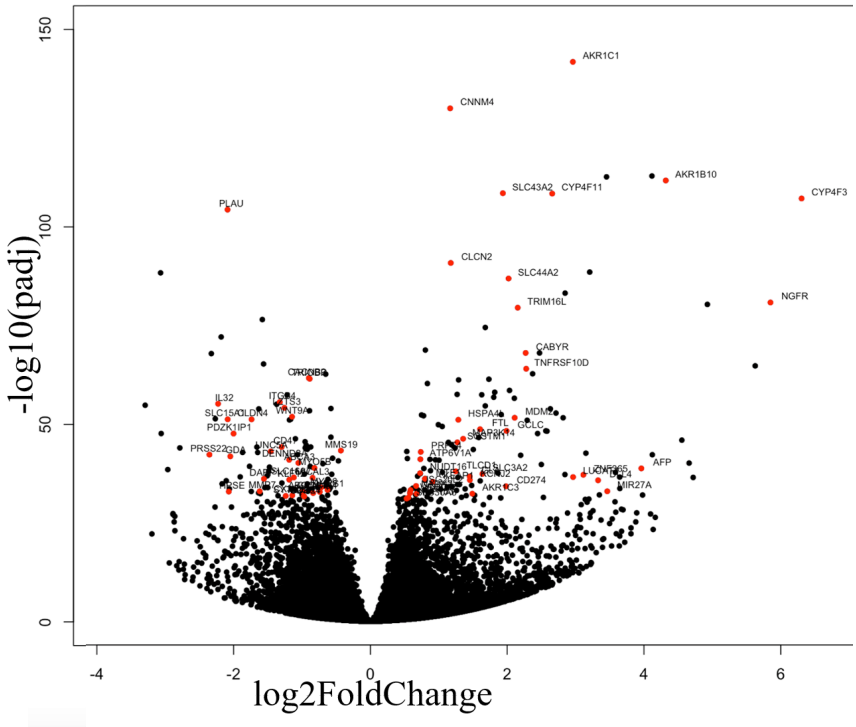

Figure 2: Volcano plot showing -$\log_{10}$(padj) vs $\log_2$FC

The red points indicate a highly differentially expressed gene that has been mentioned in previous literature.

Genetic

Introduction

We were interested in the effects FSS had on the overall gene expression of ABCC4, ABCC2, and ABCG2. These are genes for efflux transport proteins that are known to transport organic anions into the lumen (Aschauer et al., 2015).

Substrates for these proteins include many chemotherapeutics and antivirals. All three of these proteins are known to transport the camptothecin derivative, topotecan (Jedlitschky et al., 2006; Mao & Unadkat, 2015; Zhou et al., 2008). Some other notable substrates of MRP2 include the chemotherapy drugs Cisplatin and Methotrexate as well as the mycotoxin Ochratoxin A (Jedlitschky et al., 2006). BCRP also has many chemotherapeutic substrates including Irinotecan and Nilotinib (Mao & Unadkat, 2015). MRP4 substrates include cGMP and cAMP (van Aubel et al., 2002) as well as the antiviral drugs tenofovir and adefovir (Imaoka et al., 2007).

When these proteins are inhibited, it can cause a build-up of potentially nephrotoxic compounds inside the PTC, which can lead to cell death and eventually kidney damage. All three proteins are inhibited by MK-571(Chen et al., 2018; Zhou et al., 2008). More specific inhibitors include omeprazole (BCRP) (Mao & Unadkat, 2015), Sildenafil (MRP4) (Chen et al., 2018), and Azithromycin (MRP2) (Jedlitschky et al., 2006).

To verify the effects of FSS on the expression of these genes in PTCs, mRNA from cells exposed to FSS and cells that were not was compared as well as the changes between the different flow rates. Cells were exposed to either the biologically relevant rate of 0.5 dynes/cm^2 (Ferrell, Cheng, Miao, Roy, & Fissell, 2018) or one of the in-between rates of 0.25 dynes/cm^2 or 0.1 dynes/cm^2. This was done to reflect potential changes that could occur during kidney disease and to catch any gradual changes in expression between a normal FSS rate and static. RNAseq was used to measure the gene expression in human renal PTCs. **We hypothesized that gene expressions for MRP4, MRP2, and BCRP would increase to biologically relevant levels when subjected to increasing FSS.**

Methods

Cell Culture

Human embryonic kidney cells (HEK-293T, ATCC CRL-3216) were cultured in DMEM with 10% FBS and 1% Penicillin/Streptomycin. Cells were passaged every 2-3 days. Cells were kept in a 37°C, humidified incubator containing 5% CO_2.

Human renal proximal tubule epithelial cells (RPTEC-TERT1, ATCC CRL-4031) were cultured in hTERT Immortalized RPTEC Growth Kit (ATCC ACS-4007), supplemented with Geneticin (Gibco, 10131035), in phenol-red free DMEM/F-12 medium (Gibco, 11039021) according to the vendor's instructions. The cells were passaged 1-2 times per week at ratios of 1:2 or 1:3. Cells were kept in a 37°C, humidified incubator containing 5% CO_2. These cells were provided and maintained by Emily Ross.

Isolation of Genomic Material

Isolation of RNA was done with the Direct-Zol™ RNA MiniPrep Plus kit (Zymo Research, R2070). The RNA was quantified using a Qubit and the purity was checked with a 2100 Bioanalzyer.

cDNA Synthesis

The cDNA was synthesized using RevertAid First Strand cDNA Synthesis (Thermo Scientific, K1622). All RNA samples were standardized to have the same amount of starting material before being used in this kit.

PCR

The reactions were set up per the manufacturer instructions from Amplitaq (Thermo Fisher, N808-0160). Gels were made up with 2% agarose and 2.5 uL of EtBr per 100mL of gel. Thermocycler settings from the same Amplitaq protocol were used as a standard for all reactions.

Temperature (℃)	Time	Number of Cycles
95	2 min	
95	15s	32
58	30s	
72	33s	
72	5min	
4	∞	

Table 1: Thermocycler settings

Primer Design

Primers were made for the genes ABCC2, ABCC4, and ABCG2. Each had three primers found from the literature and 2-3 self-made primers. For the self-made primers, forward and reverse sequences were selected based on length (between 18-25 base pairs) and location (spanning 2 exons). They were then put through primer3 (http://bioinfo.ut.ee/primer3-0.4.0/) to determine if they were good quality. The primer3 output included the following parameters: GC content, length, melting temperature (T_M), any self complementation (ANY), 3' self complementation (3'), and 3' stability. Most primers picked had a GC% of 45-55%, a T_M between 55-70℃, T_M difference > 5℃, and a 3' < 9.

Results

RNASeq

Gene Symbol	Protein	Log_2FC	p-adjust
ABCC2	MRP2	1.433281	7.27E-22
ABCC4	MRP4	-0.985080	1.38E-33
ABCG2	BCRP	1.163821	1.17E-07

Table 2: Log_2FC and adjusted p-values for selected genes

All three genes showed some degree of significant change in expression between static and flow conditions. However, only the expression change of ABCC4 qualified as highly significant.

Primer Design

Of the nine primers obtained from the literature, only four were successful with our testing parameters. All primers for MRP4, one primer for MRP2, and none for BCRP. This is reflected below in Table 3, a "✔" indicates a primer that showed gene expression, and an "x" indicates a primer that did not. None of the self-made primers worked.

Target	BCRP			MRP2			MRP4		
Primer ID	A	B	C	D	E	F	G	H	I
RPTEC	X	X	X	✔	X	X	✔	✔	✔
HEK	X	X	X	✔	X	X	✔	✔	✔

Table 3: Results for primers from the literature

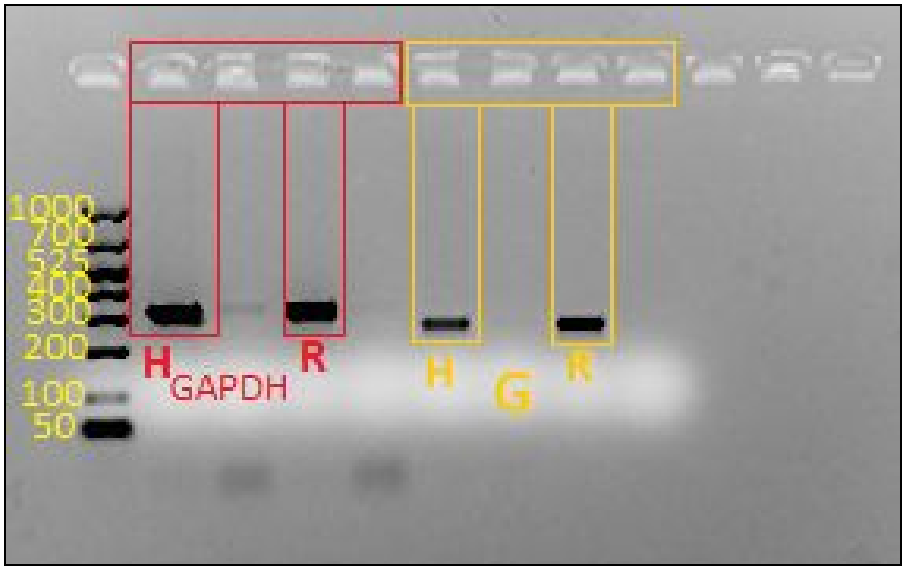

Figure 3: Gel showing expression of MRP4 (G) and GAPDH in HEK (H) and RPTEC (R) cells

GAPDH is a housekeeping gene that is highly expressed in both HEK and RPTEC cells. It is used as a control to make sure there is genomic material present, to limit false negatives. This gel was also used to establish the G primer as a positive control for later gels.

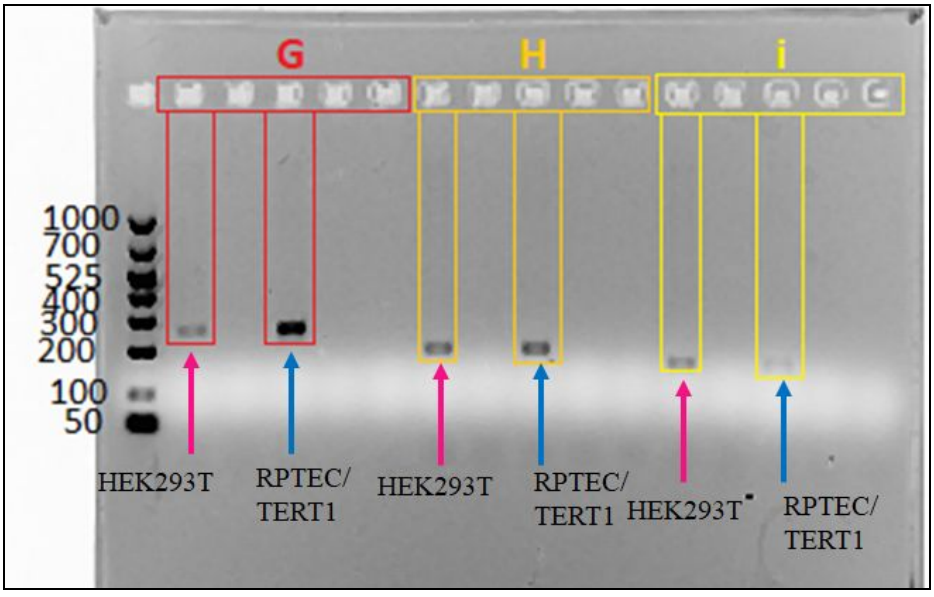

Figure 4: Gel showing the expression of MRP4 in HEK (H) and RPTEC (R) cells using the.

This is the gel for the MRP4 primers. HEK cells were used as a control due to it being a cell line with well documented gene expression level

Conclusions and Future Directions

The results of the RNAsequencing of RPTEC-TERT1 cells in static conditions versus FSS was that 10,442 genes were found to have significant change in expression levels, both upregulation and downregulation. Of those 337 had highly significant changes and of those 69 had already been reported in the literature as being related to PT structure or function. This implies that FSS is a biologically relevant environmental condition for a human PT model. The microfluidic device model that this study used is a potentially useful tool for future pharmaceutical testing. It is relatively cheap, easy to use, and mass-producible. This would allow pharmaceutical companies to streamline testing new therapies inside an *in vitro* PT model that better recapitulates the microenvironment found *in vivo* . In doing so, it would lower the risk of failure when a new therapy moves into clinical testing.

The three specific transporter protein genes that were focused on in this paper (ABCC2/4, ABCG2) all show significant differential expression between static and flow. Both ABCC2 and ABCG2 showed slight upregulation when exposed to FSS. On the other hand, ABCC4 showed a highly significant change in expression and was slightly downregulated when exposed to FSS. This is interesting as all three of these are in the same transporter family and share many classes of substrates. A future study could look into the changes in the protein levels of these three transporters to get a better understanding of what is happening to the cells when they are exposed to FSS.

Acknowledgments

I would like to thank my mentor, Emily Ross, for her patience and guidance throughout this entire process. I would also like to thank Dr. Luis Cruz-Vera for being my project director.

References

Alonso, A., Lasseigne, B. N., Williams, K., Nielsen, J., Ramaker, R. C., Hardigan, A. A., … Myers, R. M. (2017). ARNApipe: A balanced, efficient and distributed pipeline for processing RNA-seq data in high-performance computing environments. *Bioinformatics*, *33*(11), 1727–1729. https://doi.org/10.1093/bioinformatics/btx023

Anders, S., & Huber, W. (2010). Differential expression analysis for sequence count data. *Genome Biology*, *11*(10). https://doi.org/10.1186/gb-2010-11-10-r106

Aschauer, L., Carta, G., Vogelsang, N., Schlatter, E., & Jennings, P. (2015). Expression of xenobiotic transporters in the human renal proximal tubule cell line RPTEC/TERT1. *Toxicology in Vitro*, *30*(1), 95–105. https://doi.org/10.1016/j.tiv.2014.12.003

Chen, Y., Yuan, X., Xiao, Z., Jin, H., Zhang, L., & Liu, Z. (2018). Discovery of novel multidrug resistance protein 4 (MRP4) inhibitors as active agents reducing resistance to anticancer drug 6-Mercaptopurine (6-MP) by structure and ligand-based virtual screening. *PLoS ONE*. https://doi.org/10.1371/journal.pone.0205175

Chevalier, R. L. (2016). The proximal tubule is the primary target of injury and progression of kidney disease: role of the glomerulotubular junction. *American Journal of Physiology - Renal Physiology*, *311*(1), F145–F161. https://doi.org/10.1152/ajprenal.00164.2016

Dobin, A., Davis, C. A., Schlesinger, F., Drenkow, J., Zaleski, C., Jha, S., … Gingeras, T. R. (2013). STAR: Ultrafast universal RNA-seq aligner. *Bioinformatics*, *29*(1), 15–21. https://doi.org/10.1093/bioinformatics/bts635

Durinck, S., Spellman, P. T., Birney, E., & Huber, W. (2009). Mapping identifiers for the integration of genomic datasets with the R/Bioconductor package biomaRt. *Nature Protocols*, *4*(8), 1184–1191. https://doi.org/10.1038/nprot.2009.97

Ferrell, N., Cheng, J., Miao, S., Roy, S., & Fissell, W. H. (2018). Orbital Shear Stress Regulates Differentiation and Barrier Function of Primary Renal Tubular Epithelial Cells. *ASAIO Journal (American Society for Artificial Internal Organs : 1992)*, *64*(6), 766–772. https://doi.org/10.1097/MAT.0000000000000723

Heron, M. (2019). Deaths: Leading causes for 2017. *National Vital Statistics Reports*.

Hrdlickova, R., Toloue, M., & Tian, B. (2017). RNA-Seq methods for transcriptome analysis. *Wiley Interdisciplinary Reviews. RNA*, *8*(1), 10.1002/wrna.1364. https://doi.org/10.1002/wrna.1364

Hsu, R. K., & Hsu, C. (2016). The Role of Acute Kidney Injury in Chronic Kidney Disease. *Seminars in Nephrology*, *36*(4), 283–292. https://doi.org/10.1016/j.semnephrol.2016.05.005

Imaoka, T., Kusuhara, H., Adachi, M., Schuetz, J. D., Takeuchi, K., & Sugiyama, Y. (2007). Functional Involvement of Multidrug Resistance-Associated Protein 4 (MRP4/ABCC4) in the Renal Elimination of the Antiviral Drugs Adefovir and Tenofovir. *Molecular Pharmacology*, *71*(2), 619–627. https://doi.org/10.1124/mol.106.028233

Jedlitschky, G., Hoffmann, U., & Kroemer, H. K. (2006). Structure and function of the MRP2 (ABCC2) protein and its role in drug disposition. *Expert Opinion on Drug Metabolism and Toxicology*. https://doi.org/10.1517/17425255.2.3.351

King, S. M., Higgins, J. W., Nino, C. R., Smith, T. R., Paffenroth, E. H., Fairbairn, C. E., … Nguyen, D. G. (2017). 3D proximal tubule tissues recapitulate key aspects of renal physiology to enable nephrotoxicity testing. *Frontiers in Physiology*, *8*(MAR). https://doi.org/10.3389/fphys.2017.00123

Love, M. I., Huber, W., & Anders, S. (2014). Moderated estimation of fold change and dispersion for RNA-seq data with DESeq2. *Genome Biology*, *15*(12), 1–21. https://doi.org/10.1186/s13059-014-0550-8

Mao, Q., & Unadkat, J. D. (2015). Role of the Breast Cancer Resistance Protein (BCRP/ABCG2) in Drug Transport—an Update. *AAPS Journal*. https://doi.org/10.1208/s12248-014-9668-6

Marioni, J. C., Mason, C. E., Mane, S. M., Stephens, M., & Gilad, Y. (2008). RNA-seq: an assessment of technical reproducibility and comparison with gene expression arrays. *Genome Research*, *18*(9), 1509–1517. https://doi.org/10.1101/gr.079558.108

Nakamura, M., Shirai, A., Yamazaki, O., Satoh, N., Suzuki, M., Horita, S., … Seki, G. (2014). Roles of renal proximal tubule transport in acid/base balance and blood pressure regulation. *BioMed Research International*. https://doi.org/10.1155/2014/504808

Shahrbaf, F., & Assadi, F. (2015). Drug-induced renal disorders. *Journal of Renal Injury Prevention*, *4*(3), 57–60. https://doi.org/10.12861/jrip.2015.12

Snouber, L. C., Letourneur, F., Chafey, P., Broussard, C., Monge, M., Legallais, C., & Leclerc, E. (2012). Analysis of transcriptomic and proteomic profiles demonstrates improved Madin-Darby canine kidney cell function in a renal microfluidic biochip. *Biotechnology Progress*, *28*(2), 474–484. https://doi.org/10.1002/btpr.743

van Aubel, R. A. M. H., Smeets, P. H. E., Peters, J. G. P., Bindels, R. J. M., & Russel, F. G. M. (2002). The MRP4/ABCC4 Gene Encodes a Novel Apical Organic Anion Transporter in Human Kidney Proximal Tubules: Putative Efflux Pump for Urinary cAMP and cGMP. *Journal of the American Society of Nephrology*, *13*(3), 595 LP – 603. Retrieved from http://jasn.asnjournals.org/content/13/3/595.abstract

Velve-Casquillas, G., Le Berre, M., Piel, M., & Tran, P. T. (2010). Microfluidic tools for cell biological research. *Nano Today*. https://doi.org/10.1016/j.nantod.2009.12.001

Wang, Z., Gerstein, M., & Snyder, M. (2009). RNA-Seq: A revolutionary tool for transcriptomics. *Nature Reviews Genetics*. https://doi.org/10.1038/nrg2484

Yin, J., & Wang, J. (2016). Renal drug transporters and their significance in drug-drug interactions. *Acta Pharmaceutica Sinica B*. https://doi.org/10.1016/j.apsb.2016.07.013

Zhou, S.-F., Wang, L.-L., Di, Y., Xue, C., Duan, W., Li, C., & Li, Y. (2008). Substrates and Inhibitors of Human Multidrug Resistance Associated Proteins and the Implications in Drug Development. *Current Medicinal Chemistry*. https://doi.org/10.2174/092986708785132870

Appendix

Gene symbol	log2 Fold Change	p-adjust	PMID	Relationship to Proximal Tubule Cells
ABCA3	-1.053042	7.15E-41	15358727	ABCA3 gene encodes a lipid transporter critical for surfactant function at birth.
ABCC4	-0.985080	1.38E-33	17110501	Efflux transporter
AKR1B10	4.319350	1.88E-112	25577493	Mitochondrial human aldo-keto reductase with activity toward steroids and 3-keto-acyl-coa conjugates
AKR1C1	2.960844	1.60E-142	22408622	Regulation of aldo-keto reductases
AKR1C3	1.490948	4.60E-33	20126582	Reduces ketosteroids, ketoprostaglandins, and lipid aldehydes, may function as a chemical barrier
ASRGL1	-1.244455	3.57E-28	26054544	L-asparaginase and beta-aspartyl peptidase activity.
ATP6V1A	0.730308	8.29E-42	23863464	AMP-activated protein kinase regulates the vacuolar H+-atpase via direct phosphorylation of the A subunit (ATP6V1A) in the kidney
BCCIP	0.673598	4.64E-33	14726710	Regulator for the G1-S cell cycle progression and cell growth control
BMI1	0.555644	4.57E-28	24915841	Maintains redox balance
CABYR	2.270398	9.63E-69	24475127	Expressed in testes and ciliated cells
CBS	-0.901763	5.26E-30	28750410	First and rate-limiting enzyme in the transsulfuration pathway
CD47	-1.298086	6.58E-45	27259369	Mechanisms of neutrophil transmigration
CDH24	-0.967338	2.29E-32	12734196	Alpha-catenin, beta-catenin, and p120 catenin, strong cell-cell adhesion
CDKN1A	1.412203	5.57E-28	21780161	Effected by Mg levels
CLCN2	1.175479	1.50E-91	28534947	Chloride channel 2 (clc-2)
CLDN4	-1.737756	6.67E-52	20921420	Paracellular chloride channel in the kidney
CNNM4	1.166504	9.83E-131	21191290	Mg2R homeostasis

CYP4F11	2.658666	3.96E-109	28132967	Cytochrome P450 (CYP) enzymes
CYP4F3	6.304907	6.83E-108	28132967	Cytochrome P450 (CYP) enzymes
DAPP1	-1.556888	7.92E-37	10432293	A PH domain that interacts specifically with ptdins(3,4,5)P3 and ptdins(3,4)P 2
DENND2A	-1.187422	1.16E-41	20937701	The DENND2 family regulates Rab9 and lysosome distribution
DHRS1	-0.627389	4.96E-34	17579666	Cell growth and metabolism (rat)
GCLC	1.990697	5.38E-49	25170436	NRF2-responsive gene
GDA	-2.048190	1.57E-42	26316329	Guanine is deaminated to form xanthine by guanine deaminase. Xanthine is again oxidized by xanthine oxidase to form the final product, uric acid
GRAMD4	-0.739746	1.60E-33	21127500	GRAMD4 mimics p53 and mediates the apoptotic function of p73 at mitochondria.
HPSE	-2.070957	1.31E-33	21600934	Regulates the gene expression of syndecan-1, heparan sulfate reduction via its endoglycosidase activity
HSP90AA1	1.029369	1.32E-31	27036204	Oxidative stress.
HSPA4L	1.285791	8.42E-52	16923965	Suggest that Hspa4l plays a role in osmotolerance
IL32	-2.226760	7.29E-56	27302771	TIMP-1 expression induced by IL-32
ILDR2	-1.585068	3.03E-28	28461473	ILDR1 Inhibits Transepithelial Water and Solute Permeability
ISG20L2	0.668242	4.98E-35	18065403	Ribosome biogenesis at the level of 5.8 S rrna maturation, processing of the 12 S precursor rrna
ITGB4	-1.325005	2.75E-56	26221233	Epithelial-to-mesenchymal transition
KEAP1	0.912700	4.19E-36	29499228	Endogenous inhibitor for nrf2
KLF12	-1.186575	1.28E-36	16615998	Regulates expression of urea transporter (UT-A1) (ms)
LUCAT1	2.963821	2.76E-37	29371934	Bind to polycomb PRC2 complex and suppress p57 expression

MAP3K14	1.356615	5.38E-47	27620989	-
MDM2	2.109431	2.58E-52	27882940	Prevents spontaneous tubular epithelial cell death
MICAL3	-0.844816	4.28E-37	26485645	MICAL3, a protein known to interact with Rab8 and to play an important role in vesicle docking and fusion. Together, these data support a model where CC2D2A associates with NINL to provide a docking point for cilia-directed cargo vesicles
MIR27A	3.463467	1.10E-33	27351287	Directly inhibits pparγ, linked to elevated serum creatinine, proteinuria, urinary N-acetyl-β-D-glucosaminidase (NAG), and reduced estimated glomerular filtration rate (egfr).
MMP7	-1.618587	1.12E-33	28239354	Zinc- and calcium-dependent endopeptidase, biomarker for kidney fibrosis, epithelial-mesenchymal transition (EMT), transforming growth factor-beta (TGF-β) signaling, and extracellular matrix (ECM) deposition.
MMS19	-0.431714	5.35E-44	16316322	Basal transcription factors
MTF1	0.796998	7.92E-37	26708346, 10605938	Transcriptional activation of the MT-I gene in response to metals and oxidative stress.
MYO6	-0.721812	1.24E-34	11447109	Clathrin-mediated endocytosis
NADK2	0.587739	5.45E-34	29388319	Produces NADPH which is an essential co-substrate for and also acts as a molecular chaperone that activates and stabilizes alpha-aminoadipic semialdehyde synthase (AASS), the first enzyme in the lysine degradation pathway, and dienoyl-coa reductase (DECR)
NUDT16	0.726663	2.87E-38	29483298	Hydrolysis of dinucleotide cap analogs and short capped oligonucleotides
NUP153	0.555638	4.35E-32	25485891	A central function in the organization of the nucleus
PDZD7	-1.507096	4.78E-31	23055499	Paralog of harmonin and whirlin, found on

				actin filaments,a second scaffolding component of the ankle-link complex
PDZK1	-0.973729	1.81E-32	14531806	Scaffolder in brush border
PDZK1IP1	-2.000629	2.63E-48	12837682	Interactions of MAP17 with the napi-iia/PDZK1
PLAU	-2.088561	4.64E-105	25504362	Preventing calcium salt precipitation
PLD2	-0.607764	2.08E-30	29660846	Regulates angiogenin
PRSS22	-2.353522	5.69E-43	23283995	Induced by SLIGKV-NH
RAB29	-0.851171	8.09E-28	24788816	Golgi body transport , retrograde trafficking of M6PR
SLC15A1	-2.086480	6.43E-52	12237156	Mammalian peptide transporters as targets for drug delivery
SLC16A7	-1.119620	3.43E-37	23235953	Uptake of glucose into the epithelial cells
SLC30A6	0.528923	7.93E-32	30239845	Zinc transport in golgi body
SLC3A2	1.636999	4.42E-38	26739563	Rbat/SLC3A1 is responsible for cystine reabsorption in renal proximal tubules
SLC43A2	1.936986	3.15E-109	25480797	Essential amino acid transporter (Lat4)
SLC44A2	2.020303	1.32E-87	28694431	Drug transporters of the organic anion transporter (OAT) family
SQSTM1	1.272166	4.36E-46	22714671	Expressed in the cytoplasm of proximal tubules under normal conditions
SYTL2	-1.237837	1.69E-32	22820376	Synaptotagmin-Like Proteins Control Formation of a Single Apical Membrane Domain in Epithelial Cells
TNFRSF10D	2.278131	9.95E-65	28356293	Biomarker for tubulointerstitial injury
TRIM16L	2.154335	3.29E-80	27932448	Regulation of response to stimulus
TRIM65	-0.500642	2.37E-28	26347139	Autophagic response to IFN-γ.
TRIOBP	-0.886980	3.43E-62	22230192	Regulation of SGLT expression
TRPM8	-2.271139	1.10E-29	28857015	Calcium transport
UNC5A	-1.456009	8.76E-44	19211685	Netrin-1 increases proliferation and migration of renal proximal tubular epithelial cells via the UNC5B receptor

WDR26	0.578464	3.27E-33	15378603	WD40 repeat proteins play important roles in a variety of cellular functions, including cell growth, proliferation, apoptosis, and intracellular signal transduction

Table 1: List of genes that had a significant change in expression

Sequence	Direction	Length	Tm1 (°C)	Tm2 (°C)	Ta (°C)	G/C %	ANY	SELF	3' Stability (ΔG)	Primer ID	Target
TGGGATC ATGAAAC CTGGTC	Forward	20	69	63	58	50	6	3	7.9	J	BCRP
TGGATCTT TCCTTGCA GCTAA	Reverse	21	68.9	63	58	42.9	4	3	7.5		
CCTTATTG GCCTCAG GAAGAC	Forward	21	68.9	63	58	52.4	5	2	6.4	K	
GGAATCT CCATTAA TGATGTC CA	Reverse	23	67	61	56	39.1	8	3	7.9		
TCTCACA ACCATTG CATCTTG	Forward	21	68	62	57	42.9	4	2	7	L	
ATTGAGT CCTGGGC AGAAGTT	Reverse	21	70.8	65	60	47.6	4	3	6.7		
TGGCACT TTCCAATT TCAGAC	Forward	21	60.1	60.1	55.1	42.9	4	1	6.4	M	MRP2
TCTGGAA TCCGTAG	Reverse	21	59.6	59.6	54.6	47.6	5	1	6.6		

GAGATGA											
ACTTGGA CACATCT GCCATTC	Forward	21	60	60	55	47.6	6	1	6.9	N	
AAAGGAG GCCTCAG AAAACTG	Reverse	21	59.9	59.9	54.9	47.6	8	2	6.7		
AGATGCG GAAGTTA GCAGACA	Forward	21	60	60	55	47.6	3	0	6.4	O	MRP4
TCTGACTT GCAGCTT TGAGGT	Reverse	21	60.2	60.2	55.2	47.6	4	1	7.6		
AGATTGT CAGAACC CGAAGGT	Forward	21	59.9	64	59	47.6	3	2	7.9	P	
TGTAAGG CATTCCA CAGTTCC	Reverse	21	59.9	63	58	47.6	6	0	7.9		

Table 2: Primer3 output for selfmade primers

This is the results from Primer3 for each of the primers. Tm2 was calculated by a Promega calculator (https://www.promega.com/resources/tools/biomath/?calc=™) using the parameters primer concentration 200nm, Na+/K+ Concentration 50 mM, and Mg2+ Concentration 1.5mM.

Primer ID	Target	Forward	Tm (°C)	Reverse	Tm(°C)	PMID
A	BCRP	TATAGCTCAGATCATTGTCACAGTC	68	GTTGGTCGTCAGGAAGAAGAG	68.9	23153066
B		TTTCCAAGCGTTCATTCAAAAA	66.65	TACGACTGTGACAATGATCTGAGC	70.1	16917002
C		TGATAAATGGAGCACCGCGA	71.1	GCCAGTTGTAGGCTCATCCA	71.05	25505559
D	MRP2	TCCTTTGCAAGTGACCGTGA	71.1	CCTTCCTGGCCAAGTTGGAT	71.3	25505559
E		AGTGAATGACATCTTCACGTTTG	68	CTTGCAAAGGAGATCAGCAA	67.5	19131524
F		CCCTGCTGTTCGATATACCAATC	68.95	TCGAGAGAATCCAGAATAGGGAC	69.05	25986174
G	MRP4	GAGTTGCAAGGGTTCTGGGA	71.2	AAAGTCAGCACCGTGGCATA	71.25	25505559
H		GCGGCTGACGGTTACCCTCTT	75.45	TCTGATGCCTTATCCCAAAAAGCAGT	72.25	17255265
I		GGACAAAGACAACTGGTGTGCC	72	AATGGTTAGCACGGTGCAGTGG	73.8	21205825

Table 3: Primers sourced from the literature

THE UNIVERSITY OF ALABAMA IN HUNTSVILLE

David Cook <dac0010@uah.edu>

Hanna Sothers Honors Capstone

Luis Cruz-Vera <lrc0002@uah.edu> Sat, May 2, 2020 at 9:59 AM
To: "UAH biology.chair" <biology.chair@uah.edu>
Cc: David Cook <dac0010@uah.edu>, William Wilkerson <wilkerw@uah.edu>

Dear Paul,

Attached you will find Ms Sothers' Honors Capstone document. She did all her work at the HudsonAlpha institute for biotechnology. I am just the director on paper because her work was directed by a researcher that is not part of UAH, all the credits go to her and her director, Ms Emily Ross. I have reviewed her document, it is an impressive piece of work in the genetics area.

I approve this document, my digital signature is at the signatures page.

Let me know if you have any questions or concerns,

Best

Roger

--
Luis Rogelio Cruz-Vera
Associate Professor
Department of Biological Sciences
University of Alabama in Huntsville
301 Sparkman Drive
Shelby Center room 369L
Huntsville AL, 35899
Tel. 256-8246261
Fax. 256-8246305
e-mail: Luis.Cruz-Vera@uah.edu
LabWebsite: https://sites.google.com/a/uah.edu/cruz-vera-s-lab/
Facebook: https://www.facebook.com/DrCruzVeraResearchLab/

Hanna Sothers Honors Capstone Signed_CV.pdf
648K